

**New Lanthanide Tag for the Generation of Pseudocontact Shifts in DNA by Site-Specific Ligation to a Phosphorothioate Group**

Zuyan Wu<sup>#,†</sup> Michael D. Lee,<sup>#,§</sup> Thomas J. Carruthers,<sup>†</sup> Monika Szabo,<sup>§</sup> Matthew L. Dennis,<sup>§</sup> James D. Swarbrick<sup>\*,§</sup> Bim Graham,<sup>\*,§</sup> Gottfried Otting<sup>\*,†</sup>

<sup>†</sup>Research School of Chemistry, Australian National University, Canberra, ACT 2601, Australia

<sup>§</sup>Medicinal Chemistry, Monash Institute of Pharmaceutical Sciences, Monash University, Parkville, VIC 3052, Australia

<sup>#</sup> The first two authors contributed equally

<sup>\*</sup>To whom correspondence should be addressed.

Gottfried Otting, Research School of Chemistry, Australian National University, Canberra, ACT 2605, Australia

Fax: +61-2-61250750

E-mail: gottfried.otting@anu.edu.au

Bim Graham, Medicinal Chemistry, Monash Institute of Pharmaceutical Sciences, Parkville, VIC 3052, Australia

Fax: +61-3-99039543

E-mail: bim.graham@monash.edu

James D Swarbrick, Medicinal Chemistry, Monash Institute of Pharmaceutical Sciences, Parkville, VIC 3052, Australia

Fax: +61-3-99039543

E-mail: james.swarbrick@monash.edu

Dedicated to the memory of Professor Leone Spiccia

## Abstract

Pseudocontact shifts (PCS) generated by paramagnetic lanthanides provide a rich source of long-range structural restraints that can readily be measured by nuclear magnetic resonance (NMR) spectroscopy. Many different lanthanide-binding tags have been designed for site-specific tagging of proteins, but established routes for tagging DNA with a single metal ion rely on difficult chemical synthesis. Here we present a simple and practical strategy for site-specific tagging of inexpensive phosphorothioate (PT) oligonucleotides. Commercially available PT oligonucleotides are diastereomers with *S* and *R* stereo-configuration at the backbone PT site. The respective *S<sub>P</sub>* and *R<sub>P</sub>* diastereomers can readily be separated by HPLC. A new alkylating lanthanide-binding tag, **C10**, was synthesized that delivered quantitative tagging yields with both diastereomers. PCSs were observed following ligation with the complementary DNA strand to form double-stranded DNA duplexes. The PCSs were larger for the *S<sub>P</sub>* than the *R<sub>P</sub>* oligonucleotide and good correlation between back-calculated and experimental PCSs was observed. The **C10** tag can also be attached to cysteine residues in proteins, where it generates a stable thioether bond. Ligated to the A28C mutant of ubiquitin, the tag produced excellent fits of magnetic susceptibility anisotropy ( $\Delta\chi$ ) tensors, with larger tensors than for the tagged PT oligonucleotides, indicating residual tag mobility following ligation with a PT group.

## INTRODUCTION

Pseudocontact shifts (PCS) generated by paramagnetic lanthanide ions provide valuable long-range structural restraints for determinations of the 3D structures of proteins and protein-ligand complexes.<sup>1-4</sup> PCS measurements would be particularly attractive for studying the structure of DNA and RNA by NMR spectroscopy, as the proton density of oligonucleotides is less than in proteins, limiting the potential to derive structural restraints from nuclear Overhauser effects (NOE). To the best of our knowledge, however, generation of PCSs in oligonucleotides by a covalently attached paramagnetic metal tag has never been reported. This can be attributed to the stringent set of requirements any suitable tag must fulfil, including a sufficiently rigid tether between metal ion and oligonucleotide to prevent the averaging of positive and negative PCSs, and a well-defined metal position to allow the fitting of a single magnetic susceptibility anisotropy ( $\Delta\chi$ ) tensor, which is required to derive meaningful structural restraints from the PCSs. Well-defined metal positions are also required to perform EPR measurements of nanometer distances between two site-specifically attached  $\text{Gd}^{3+}$  ions,<sup>5</sup> which would be very attractive for structure analysis of large RNA molecules.

Many lanthanide tags have been developed for site-specific tagging of proteins. Most tags target the thiol group of cysteine residues, most often reacting with formation of a disulfide bond.<sup>3,4,6</sup> Alternatively, electrophilic tags have been designed that form a thioether linkage, which is chemically more stable and also produces a shorter linker between the sulfur atom and the lanthanide ion.<sup>7-11</sup>

Attaching lanthanide-binding tags to DNA or RNA is more difficult because native nucleotides contain no thiol groups. Obviously, this limitation does not hold for synthetic DNA fragments, which can be furnished with a wide variety of non-natural functional groups.<sup>12</sup> Unfortunately, commercially available oligonucleotides with chemically modified nucleotide bases tend to include long flexible linkers. As the sign of PCSs can be positive or negative, depending on the orientation of the  $\Delta\chi$  tensor of the lanthanide complex relative to the macromolecule carrying the tag, averaging between different orientations due to linker flexibility greatly decreases the magnitude of observable PCSs all the way to zero. In addition, DNA with chemically modified nucleotides tends to be prohibitively expensive in the amounts needed for NMR spectroscopy. Finally, labeling DNA with lanthanides can be problematic because

lanthanide ions readily bind to the phosphodiester backbone of DNA<sup>13</sup> and catalyze hydrolytic cleavage.<sup>14</sup> It is thus important that any lanthanide complex protects the lanthanide ion from potential release due to direct contacts with the phosphodiester backbone of the DNA. These criteria are best fulfilled by kinetically inert lanthanide complexes, such as those of the well-known macrocyclic ligand 1,4,7,10-tetraazacyclododecane-1,4,7,10-tetraacetic acid (DOTA).

Phosphorothioate (PT) groups present a popular, commercially available and inexpensive modification of DNA. This modification is useful in biochemical experiments, as the sulfur atom confers resistance to nucleases<sup>15</sup> without interfering with base pairing. A single PT group can be positioned between any two nucleotides with minimal impact on the DNA structure. For the purpose of site-specific DNA labeling, there is evidence that the sulfur atom in the PT group rather than the non-bridging oxygen accumulates a negative charge at neutral pH,<sup>16</sup> suggesting reactivity akin to the thiolate of a cysteine residue.

In practice the reactivity of a PT group is less than that of a cysteine thiolate and alkylated PT groups are also less stable chemically. For example, alkylation of single internal PT diesters in DNA has been shown to require a number of hours at 50 °C in the pH range 5-8. The resulting PT triesters are relatively stable at neutral pH, but prone to base-catalyzed hydrolysis at room temperature under alkaline conditions, leading to classical phosphodiesters and loss of the chemical modification. Incorporation of the alkylated PT groups within double-stranded DNA offers some protection against hydrolysis.<sup>17</sup> This alkylation approach has recently been used to label a 13-mer DNA fragment containing a PT group with the nitroxide tag iodoacetamide-PROXYL for the generation of paramagnetic relaxation enhancements (PRE) in NMR spectra. The tagged DNA enabled the observation of PREs in the *Sulfolobus solfataricus* single-stranded DNA binding protein.<sup>18</sup>

An unavoidable complication associated with PT linkages in DNA arises from the chirality of the phosphorus atom. Phosphorothioates in commercially available DNA are not produced with stereo-selectivity. NMR spectra of the resulting diastereomers would thus display peak doubling, calling for separation of the diastereomers prior to tagging and NMR analysis. The two diastereomers, commonly denoted  $R_P$  and  $S_P$  (Figure 1a) can be distinguished chemically by different hydrolysis rates with snake venom phosphodiesterase, which digests the  $R_P$  diastereomer orders of magnitude faster than the  $S_P$  diastereomer.<sup>19,20</sup>

Chromatographic separation of the  $R_P$  and  $S_P$  diastereomers may seem challenging, if there is only a single PT group in the entire nucleotide sequence. Nonetheless, phosphorothioate oligoribonucleotides with up to 25 nucleotides have been successfully separated by strong anion-exchange and reverse-phase HPLC protocols.<sup>21</sup>

In the present work we separated the  $R_P$  and  $S_P$  diastereomers of a 14-mer oligonucleotide with a single PT group by reverse-phase HPLC using a conventional C18 column. The individual diastereomers were tagged with a new alkylating lanthanide-binding tag (**C10**), combined with the complementary strand to form duplex DNA (Figure 1b), and PCSs were observed in 2D NOESY spectra. In addition, the performance of the **C10** tag was evaluated by NMR spectroscopy following attachment to the A28C mutant of human ubiquitin. To the best of our knowledge, this is the first time that pseudocontact shifts have been generated in a DNA or RNA oligomer by covalent attachment of a paramagnetic metal ion tag.

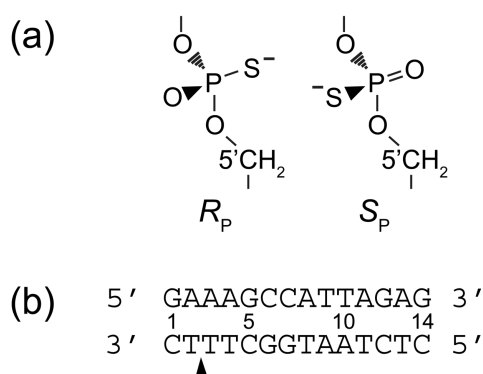


**Figure 1.** a) Phosphorothioate moiety in the phosphodiester backbone of oligonucleotides. The stereo-configurations  $R_P$  and  $S_P$  are shown. b) Nucleotide sequence of the 14-mer DNA duplex used in the present study. The DNA corresponds to the DNA-recognition motif of the *Antennapedia* homeodomain in *Drosophila*. The complementary strand without the PT modification is written as the sense strand as in previous publications<sup>22,23</sup> and the base pairs are numbered 1-14. The phosphorothioate group is between T<sub>2</sub> and T<sub>3</sub> (highlighted by an arrow).

## RESULTS

**Sample preparation.** Separation of NMR quantities of the  $R_P$  and  $S_P$  diastereomers proved straightforward with a semi-preparative scale C18 column. Baseline separation was achieved between the two diastereomers (Figure 2). The configurations of the two separated diastereomers were determined by enzymatic digestion with snake venom phosphodiesterase, which is known to cleave  $R_P$  but not  $S_P$  diastereomers. HPLC analysis following SVP digestion of the individual diastereomers showed that the first eluate corresponded to the  $R_P$  configuration as it was digested more quickly, in agreement with literature results<sup>21</sup> (Figure S4).

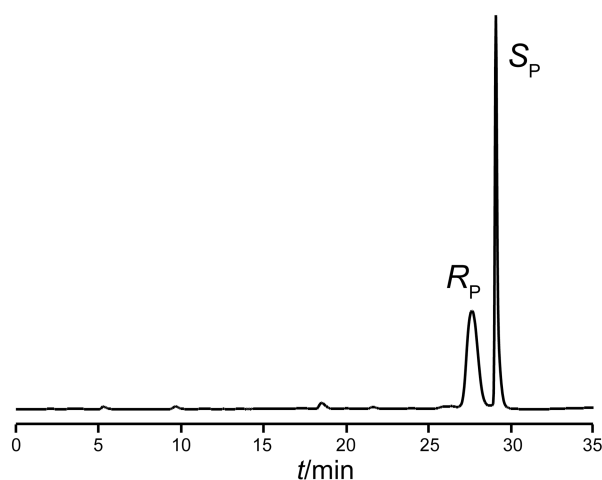


**Figure 2.** HPLC separation of  $R_P$  and  $S_P$  diastereomers. Absorbance of the HPLC eluent was measured at 260 nm. Conditions: C18 HPLC column; flow rate 3 mL/min with a linear MeOH gradient (15–100%) in 40 mM ammonium carbonate (pH 8.0).

Initial attempts to tag the PT oligonucleotides with compounds containing activated disulfide bonds (such as the **C1** tag<sup>22</sup>) failed. As a previous report showed successful alkylation of PT oligonucleotides with iodoacetamide-PROXYL,<sup>18</sup> we produced the **C10** tag (Figure 3), which is a cyclen-based tag featuring an alkylating group akin to that found in the recently reported **CLaNP-9** tag of Liu et al.<sup>9</sup> Like earlier cyclen tags,<sup>24-26</sup> it contains chiral phenylethylacetamide groups to populate a single stereoisomer of the lanthanide complex.

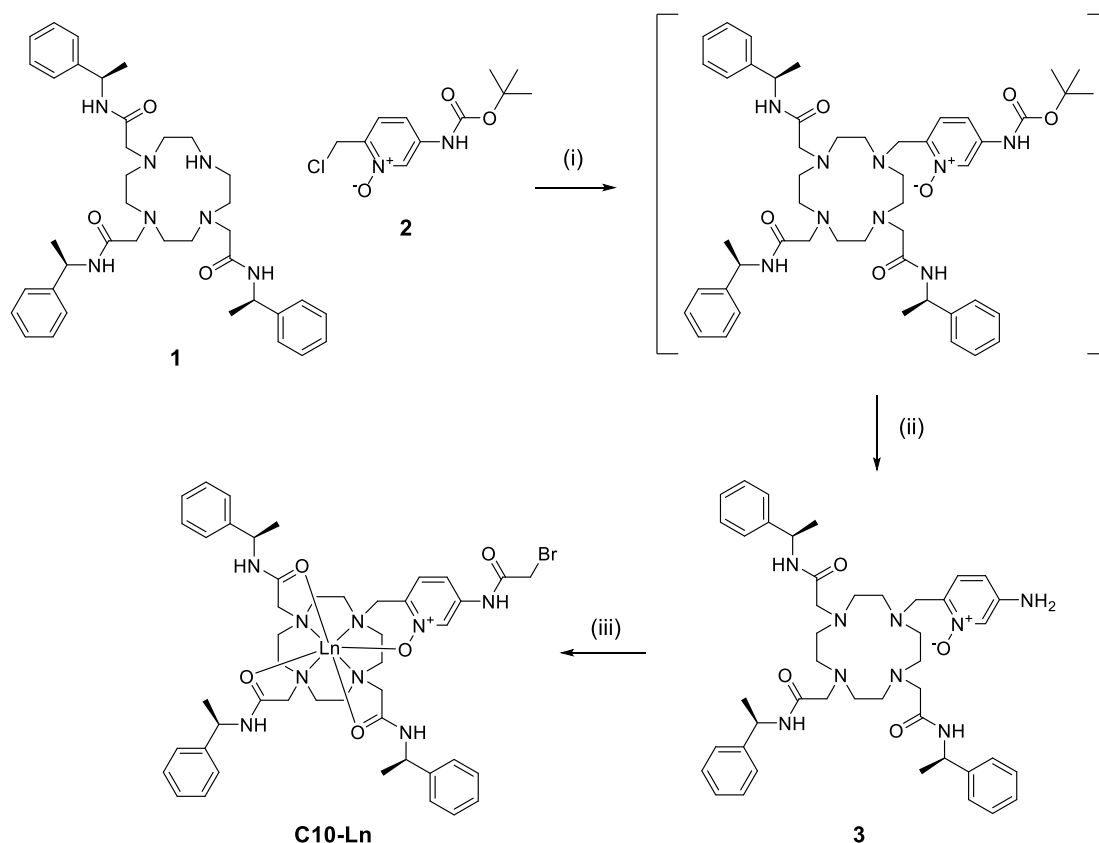


**Figure 3.** Synthesis of lanthanide complexes of **C10**. Reagents and conditions: (i) DIPEA, CH<sub>3</sub>CN, DMF, 80 °C, 1 h; (ii) triethylsilane, TFA, CH<sub>2</sub>Cl<sub>2</sub>, RT, 2 h, 46% (over two steps); (iii) Ln(OAc)<sub>3</sub>, DMF, RT, 1 h, DIPEA, bromoacetyl bromide, RT, 10 min, 34%.

Ligation reactions using a five-fold excess of tag (loaded with either Tb<sup>3+</sup>, Tm<sup>3+</sup> or Y<sup>3+</sup>) produced tagged DNA in practically quantitative yield in an overnight reaction (Figure S5). The tagged product proved to be sensitive to hydrolysis during lyophilization in the presence of ammonium carbonate. Following removal of the ammonium carbonate by ultrafiltration with water, however, the product was stable during lyophilization and no noticeable degradation of the tagged duplex DNA was observed after many days of NMR measurements at 25 °C.

**PCS measurements.** The <sup>1</sup>H-NMR resonances of the 14-mer DNA were assigned by 2D NOESY spectra. Spectra were recorded not only for the DNA duplexes with a **C10** tag, but also for a duplex made from oligonucleotides without PT modification. The chemical shifts of the DNA samples with diamagnetic Y<sup>3+</sup> tag were very similar to those of the untagged DNA. The largest chemical shift difference observed between the **C10**-Y<sup>3+</sup>-tagged DNA and the equivalent conventional DNA

duplex containing no PT group was 0.005 ppm, indicating that the tag did not significantly alter the DNA structure. All paramagnetically tagged DNA duplexes displayed paramagnetic shifts and PCSs were observed throughout the duplexes (Tables S1 and S2). No NOE cross-peaks of H1' or base protons were lost due to paramagnetic relaxation enhancements in the samples tagged with the **C10**-Tm<sup>3+</sup> tag, but paramagnetic relaxation enhancement (PRE) effects led to weaker cross-peaks observed in the samples tagged with the Tb<sup>3+</sup>-loaded **C10** tag, as the magnetic susceptibility of a Tb<sup>3+</sup> ion is greater than that of a Tm<sup>3+</sup> ion.

The resonance assignments of the paramagnetic samples were aided by the fact that PCSs produced by Tb<sup>3+</sup> and Tm<sup>3+</sup> displaced the cross-peaks in generally opposite directions (Figures 4 and 5). Notably, however, the PCSs generated by the Tb<sup>3+</sup>- and Tm<sup>3+</sup>-loaded tags were not simply proportional to each other. This effect is expected for slightly different  $\Delta\chi$  tensor orientations and is more obvious in NOESY than in HSQC spectra as the <sup>1</sup>H spins producing NOESY cross-peaks are much further apart than the nuclei producing HSQC cross-peaks. Therefore, the  $\Delta\chi$  tensor determinations were mostly based on PCSs measured for clearly resolved cross-peaks as in the spectral regions shown in Figures 4 and 5. At least 12 PCSs were determined in this way for each metal ion and DNA sample (Tables S1 and S2). On average, the PCS values for the *S<sub>P</sub>* isomer were greater in magnitude than for the *R<sub>P</sub>* isomer. For both isomers, measurable PCSs were observed along the entire length of the DNA.

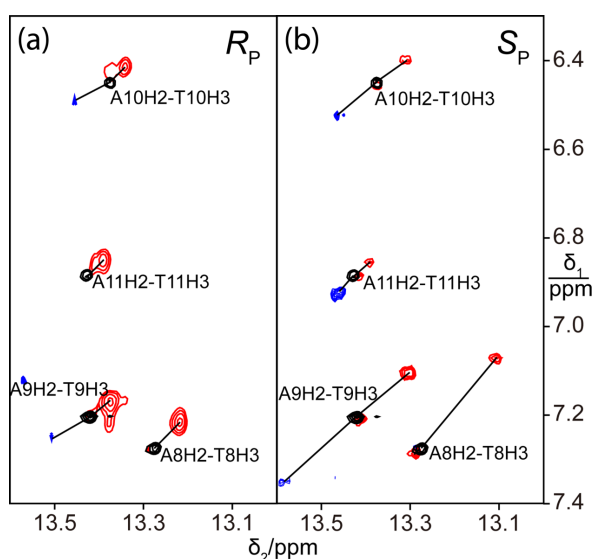




**Figure 4.** Selected spectral regions of  $^1\text{H}$ - $^1\text{H}$  NOESY spectra of tagged 14-mer DNA duplexes made with  $R_P$  and  $S_P$  DNA strands. Each panel shows the superimposition of three spectra, corresponding to samples containing **C10** tags loaded with  $\text{Y}^{3+}$  (black),  $\text{Tb}^{3+}$  (blue) and  $\text{Tm}^{3+}$  (red). All spectra were recorded of 50  $\mu\text{M}$  DNA duplexes in 50 mM sodium phosphate buffer, pH 7.4, at 10  $^\circ\text{C}$  on a 800 MHz NMR spectrometer. Selected diamagnetic cross-peaks are labeled with their resonance assignments and connected by lines with their paramagnetic counterparts. The spectral region shown contains cross-peaks with imino proton resonances. The greater sensitivity of the spectra with **C10**- $\text{Tm}^{3+}$  than **C10**- $\text{Tb}^{3+}$  tag allowed plotting more contour lines. (a) Spectra of duplexes made with  $R_P$  DNA strands. (b) Spectra of duplexes made with  $S_P$  DNA strands.

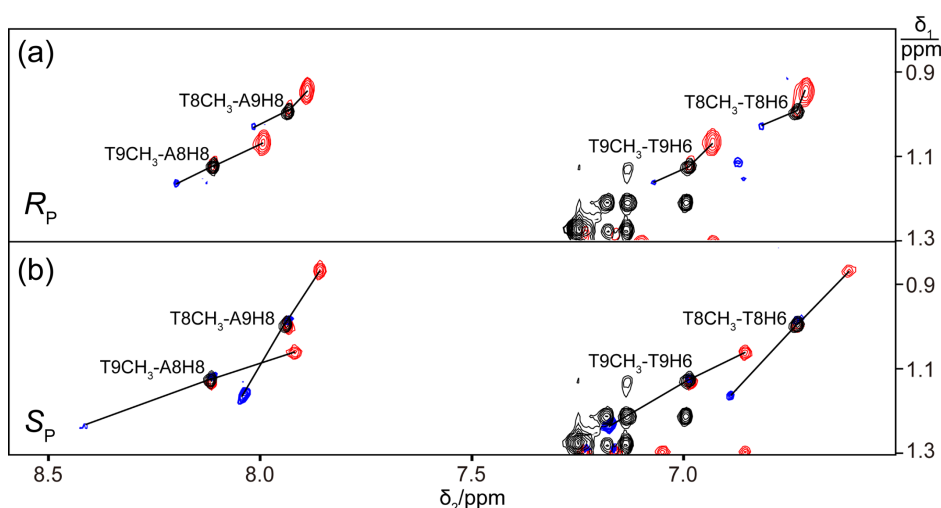


**Figure 5.** Same as Figure 4, except for cross-peaks between thymidine methyl resonances and H6 protons.

**$\Delta\chi$  Tensors.** The PCSs observed for the  $R_P$  and  $S_P$  DNA duplexes were used to fit  $\Delta\chi$  tensors to a model of standard B-type DNA. Table 1 shows the parameters of the fitted  $\Delta\chi$  tensors that were produced using the  $\text{Tm}^{3+}$  and  $\text{Tb}^{3+}$  data sets with a common metal position, Figure 6 shows the correlations between back-calculated and experimental PCSs, and Figure 7 shows the metal position obtained with these fits. The quality factors obtained for the  $\Delta\chi$  tensor fits obtained for the  $R_P$  isomer were poor, indicating that the tag failed to position the metal ion in a unique location and

orientation relative to the DNA. Smaller than expected PCSs (Figure 6a) and poor quality factors are a hallmark of flexible lanthanide tags.<sup>28</sup> In contrast, the  $S_P$  isomer displayed larger PCSs and the  $\Delta\chi$  tensor fits produced better  $Q$  factors and better correlations between back-calculated and experimental PCSs (Figure 6b). In the B-DNA model of Figure 7, the  $S_P$  diastereomer projects the sulfur towards the minor groove, whereas the  $R_P$  diastereomer directs the sulfur towards the major groove. The metal positions indicated by the  $\Delta\chi$ -tensor fits are in agreement with this relative orientation, although the position of the metal ion is highly uncertain in the case of the  $R_P$  diastereomer.

**Table 1.**  $\Delta\chi$  Tensor parameters of **C10**-tagged 14-mer  $R_P$  and  $S_P$  diastereomers, loaded with  $Tb^{3+}$  or  $Tm^{3+}$ .<sup>a</sup>

DNA and tag	$\Delta\chi_{ax}$	$\Delta\chi_{rh}$	$Q$ factor
$R_P$ - <b>C10</b> - $Tm^{3+}$	5.9	3.7	0.52
$R_P$ - <b>C10</b> - $Tb^{3+}$	-6.1	-2.9	0.26
$S_P$ - <b>C10</b> - $Tm^{3+}$	-3.3 (1.7)	-0.3 (0.8)	0.09
$S_P$ - <b>C10</b> - $Tb^{3+}$	-9.3 (1.3)	-3.6 (0.6)	0.05

<sup>a</sup>  $\Delta\chi$  tensor parameters in units of  $10^{-32} \text{ m}^3$ . The fits were performed using the program Numbat.<sup>27</sup> Uncertainty ranges (in brackets) were derived from Monte-Carlo simulations, repeating the fits 100 times while randomly omitting 10% of the PCSs. In the case of the  $R_P$  diastereomer, the quality of the fit was insufficient to produce meaningful uncertainty ranges. The quality factors  $Q$  were calculated as the RMSD of back-calculated minus experimental PCSs divided by the root-mean-square of the experimental PCSs.

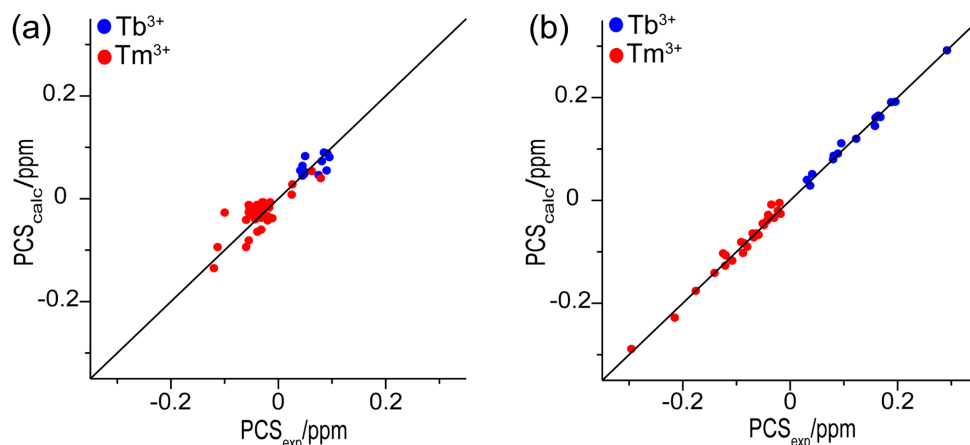


**Figure 6.** Correlation between back-calculated and experimental pseudocontact shifts of  $R_P$  and  $S_P$  isomers of the 14-mer DNA duplex ligated with the **C10** tag. Blue and red points mark the PCSs obtained with tags loaded with  $Tb^{3+}$  and  $Tm^{3+}$ , respectively. (a) Correlation plot for the  $R_P$  isomer. (b) Correlation plot for the  $S_P$  isomer.

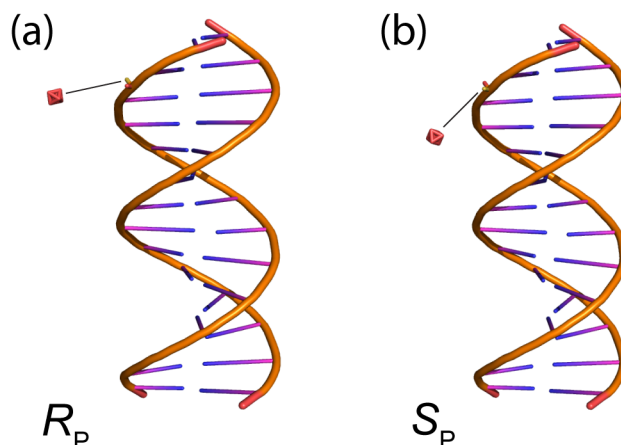


**Figure 7.** Cartoon representation of 14-mer DNA highlighting the metal positions obtained by fitting  $\Delta\chi$  tensors to a standard B-type DNA. The metal positions are identified by red octahedrons. The bond to the sulfur atom of the phosphorothioate group is shown as a yellow line, and the position of the sulfur atom is also marked by a black line indicating the distance between the sulfur atom and the metal ion. (a) Fit using the PCSs measured for the  $R_P$  isomer. The metal is about 15 Å from the sulfur atom of the PT group. (b) Fit using the PCSs measured for the  $S_P$  isomer. The fitted metal position is located about 11 Å from the sulfur atom of the PT group.

**Ligation of ubiquitin A28C with the C10 tag.** To probe the degree of immobilization of the **C10** tag, we compared the magnitudes of the  $\Delta\chi$  tensors determined for the DNA (Table 1) with  $\Delta\chi$  tensors determined with the **C10** tag attached to a protein. The tag reacts with cysteine residues by formation of a stable thioether bond. Using the A28C mutant of  $^{15}\text{N}$ -labeled human ubiquitin tagged with **C10** loaded with either  $\text{Tm}^{3+}$ ,  $\text{Tb}^{3+}$ ,  $\text{Yb}^{3+}$ , or  $\text{Y}^{3+}$ , significant PCSs were measured (Figure S6). The  $\Delta\chi$  tensor fits yielded  $\Delta\chi_{\text{ax}}$  values much larger than for either DNA diastereomer (Table S3), indicating that the **C10** tag is less well immobilized on the DNA. In the case of the ubiquitin A28C mutant, the tag delivered excellent correlations between back-calculated and experimental PCSs (Figure S7) and the  $\Delta\chi$  tensor fit positioned the metal ion 9.6 Å from the  $\text{C}^\alpha$  atom of residue 28, in good agreement with the chemical structure of the tag (Figure S8). The **C10** tag produced larger  $\Delta\chi$  tensors than those of the **C1** tag bound to the same ubiquitin mutant,<sup>24</sup> which may be attributed to the smaller number of rotatable bonds in the linker between the protein backbone and the metal ion. Remarkably, the **C10-Yb<sup>3+</sup>** tag allowed observation of PCSs even for the amide group of the residue it was attached to, and these PCSs were in excellent agreement with back-calculated values. These properties make the tag a promising tool for interrogating structural details in the immediate proximity of the tag.

## DISCUSSION

While dozens of lanthanide tags have been developed to measure PCSs in proteins, these tags are generally not suitable for DNA as they target free thiol groups or rely on the incorporation of unnatural amino acids. As carbon-bound thiol groups do not occur in natural nucleotides, it is attractive to use sulfur chemistry for site-specific ligation reactions. Unfortunately, however, chemical synthesis of unnatural nucleotides containing thiol groups or groups for other bio-orthogonal reactions is expensive. In an alternative strategy, Gochin showed that PCSs can also be generated in DNA by a  $\text{Co}^{2+}$  ion that binds to chromomycin- $\text{A}_3$  molecules, which in turn bind to GC steps in DNA with 2:1 stoichiometry,<sup>29</sup> but this approach is limited by the requirement of specific nucleotide sequences.

For oligonucleotides, a PT group arguably represents the most readily

available chemical modification. Although PT groups in DNA have been proposed to assume thioate character at neutral pH,<sup>16</sup> we found derivatization with a tag to be less straightforward than for cysteine residues in proteins. Most notably, in our hands the PT group was not amenable to disulfide exchange reactions with tags containing activated disulfide bonds such as in the **C1** tag. The alkylating **C10** tag, however, allowed site-specific tagging of the DNA on the PT group with quantitative yields. It is interesting to note that metal ions with higher valency have been reported to catalyze alkylation of phosphorothioate DNA.<sup>30</sup> It is not clear whether the limited accessibility of the lanthanide ion in the **C10** tag would still allow this catalytic effect to occur.

In principle, phosphorothioates can be alkylated either on sulfur or oxygen atoms. Careful studies have shown, however, that alkylation of phosphorothioate diesters preferentially produces *S*-alkylated rather than *O*-alkylated products,<sup>31</sup> in agreement with a greater charge on the sulfur<sup>16</sup> and the generally greater nucleophilicity of sulfur. In agreement with this result, the fitted metal positions observed in the present work were closer to the thioate than to the non-bridging oxygen atoms.

The metal ion is better immobilized in the *S<sub>P</sub>* than *R<sub>P</sub>* diastereomer, as indicated by larger PCSs, better *Q* factors of the  $\Delta\chi$  tensor fits and a metal position in good agreement with the covalent structure of the tag (Figures 6 and 7). To explain the better performance of the *S<sub>P</sub>* diastereomer, we note that the  $\Delta\chi$ -tensor fit for the *S<sub>P</sub>* diastereomer positioned the metal ion within about 7 Å of a non-bridging oxygen of the following phosphodiester (Figure 7b). Compared with the *R<sub>P</sub>* diastereomer, the *S<sub>P</sub>* diastereomer may promote a favorable interaction of the positively charged **C10**-Ln<sup>3+</sup> tag with the negatively charged phosphodiester backbone. Nonetheless, the tag must retain a considerable degree of flexibility, as the  $\Delta\chi$  tensors obtained for ubiquitin ligated with the **C10** tag were significantly larger, indicating better immobilization of the tag on the protein than on the DNA. Importantly, however, even if the tag remains flexible to some degree, our work shows that good correlations between back-calculated and experimental PCSs can be achieved (Figure 6b). The resulting effective  $\Delta\chi$  tensor thus offers a basis for meaningful structural restraints.

In conclusion, alkylation of a phosphorothioate group with a lanthanide tag provides a viable and generally applicable route to generate PCSs in DNA, even

though the phosphodiester backbone of DNA is more solvent exposed than the sulfur atom of a cysteine residue in a typical  $\alpha$ -helix of a protein. We anticipate that this approach will be useful for studies of protein-DNA interactions as well as for studies of RNA structure, following incorporation of deoxyribophosphorothioate linkages into the RNA to avoid phosphodiester bond cleavage.<sup>32</sup> Finally, the stability of thioether bonds also makes the **C10** tag attractive for protein structure analysis, where it is particularly promising for investigating structural details in the immediate proximity of the tag.

## EXPERIMENTAL SECTION

**DNA Phosphorothioate Oligonucleotides.** All oligonucleotides were purchased from Integrated DNA Technologies (IDT) and dissolved in H<sub>2</sub>O to make 10 mM stock solutions. The purchased oligonucleotides were desalted but otherwise used as received. The oligonucleotide d(CTCTAATGGCTT\*TC) was ordered, where the star denotes a single PT group between nucleotides T<sub>2</sub> and T<sub>3</sub> in the numbering of Figure 1. The complementary strand was ordered without a PT modification.

**Separation and Identification of *R<sub>P</sub>* and *S<sub>P</sub>* Diastereomers.** The *R<sub>P</sub>* and *S<sub>P</sub>* diastereomers of the PT oligonucleotides were separated by reverse-phase HPLC using a linear MeOH gradient (15–100%) in 40 mM ammonium carbonate (pH 8.0) on a semi-preparative C18 HPLC column (X-Bridge). The oligonucleotides eluted at about 35% MeOH. The buffer of the DNA fractions was exchanged for water by ultrafiltration using an Omega membrane (Pall Corporation, Port Washington, NY, USA) with 1 kDa molecular weight cutoff. The *R<sub>P</sub>* and *S<sub>P</sub>* diastereomers were identified by digesting the same concentrations of the two separated oligonucleotides with snake venom phosphodiesterase (SVP) in 20 mM Tris-HCl buffer (pH 8) containing 15 mM MgCl<sub>2</sub>. The reactions (each in a volume of 50  $\mu$ L) were terminated by adding 100 mM EDTA (10  $\mu$ L). The resulting mixtures were analyzed by reverse-phase HPLC on an analytical C18 column, using 50 mM triethylammonium acetate (TEAA) as buffer A and 80% CH<sub>3</sub>CN/20% TEAA as buffer B.

**Materials and Reagents Used in Tag Synthesis.** 2,2',2''-(1,4,7,10-Tetraazacyclododecane-1,4,7-triyl)tris-(*N*-((*R*)-1-phenylethyl)acetamide) (**1**) (Figure 3)<sup>24</sup> and 5-((*tert*-butoxycarbonyl)amino)-2-(chloromethyl)pyridine 1-oxide (**2**)<sup>9</sup> were prepared following literature procedures. All other starting materials, reagents and

solvents were obtained from commercial suppliers and were of general reagent or analytical grade and used without further purification. Instrumentation used in tag characterization is described in the Supporting Information.

**Tag Synthesis.** A solution of **1** (137 mg, 0.21 mmol), **2** (83 mg, 0.32 mmol) and *N,N*-diisopropylethylamine (DIPEA, 73  $\mu$ L, 0.42 mmol) in CH<sub>3</sub>CN (4 mL) and *N,N*-dimethylformamide (DMF, 2 mL), was heated to 80 °C for 1 h. After cooling to room temperature, the reaction was concentrated under reduced pressure and the resulting residue washed with CHCl<sub>3</sub> (50 mL) and NaOH (1 M, 50 mL). The organic phase was further washed with H<sub>2</sub>O (50 mL) and brine (50 mL), before being dried with anhydrous MgSO<sub>4</sub> and concentrated under reduced pressure. Triethylsilane (102  $\mu$ L, 0.64 mmol) and CH<sub>2</sub>Cl<sub>2</sub> (3 mL) were added to the resulting residue, followed by trifluoroacetic acid (TFA, 3 mL); the solution was stirred at room temperature for 2 h. Volatile solvents were removed by blowing a gentle stream of N<sub>2</sub> over the open reaction vessel, before the crude residue was purified by reverse-phase HPLC (0.1% TFA and a 5–100% CH<sub>3</sub>CN gradient over 30 min on a C8 preparative column). Fractions containing pure product were lyophilized to yield **3** as a white solid. Yield 131 mg (46%, based on a pentatrifluoroacetate salt). <sup>1</sup>H NMR (400 MHz, D<sub>2</sub>O)  $\delta$  7.64 (br s, 1H), 7.33 (m, 12H), 7.23 (m, 5H), 6.83 (br s, 1H), 4.89 (m, 2H), 4.74 (m, 1H, CH), 3.99 (br s, 2H, CH), 3.73–2.82 (br m, 24H), 1.43 (m, 6H, CH<sub>3</sub>), 1.33 (br d, *J* = 6.3 Hz, 3H, CH<sub>3</sub>). <sup>13</sup>C NMR (101 MHz, D<sub>2</sub>O)  $\delta$  147.27 (HMBC, C), 143.60 (C), 143.43 (C), 129.76 (br, CH), 128.87 (CH), 128.78 (CH), 127.54 (CH), 127.39 (CH), 126.06 (CH), 125.92 (CH), 125.85 (CH), 125.61 (CH), 54.42 (br, CH<sub>2</sub>), 50.01 (CH), 49.60 (br, CH), 21.54 (CH<sub>3</sub>), 21.31 (CH<sub>3</sub>). HRMS (ESI) *m/z* calcd [M+H]<sup>+</sup> C<sub>44</sub>H<sub>60</sub>N<sub>9</sub>O<sub>4</sub>: 778.4763, found: 778.4767. Note: The <sup>1</sup>H-NMR spectrum of the trifluoroacetate salt of **3** in D<sub>2</sub>O shows extensive broadening of the signals corresponding to the cyclen ring and adjacent pendant arm protons. The <sup>13</sup>C-NMR spectrum displays only a single broad CH<sub>2</sub> signal, despite the presence of 12 distinct CH<sub>2</sub> environments within its structure. Several quaternary carbons are not observed, even in 2D [<sup>13</sup>C,<sup>1</sup>H]-HMBC experiments, possibly due to a combination of protonation of nearby nitrogen atoms and chemical exchange.

Compound **3** (5 mg, 0.004 mmol) and Y(OAc)<sub>3</sub>·6H<sub>2</sub>O (2 mg, 0.008 mmol) were dissolved in DMF (50  $\mu$ L) and stirred at room temperature for 1 h, after which LC-MS analysis indicated complete complexation. The reaction was then diluted with DMF (100  $\mu$ L) before the addition of DIPEA (10  $\mu$ L, 0.06 mmol) and bromoacetyl

bromide (2.6  $\mu$ L, 0.03 mmol). The reaction was left at room temperature for 5 min before a second addition of bromoacetyl bromide (2.6  $\mu$ L, 0.03 mmol), after which analytical HPLC analysis indicated complete reaction of the aniline complex. The crude reaction was then purified by reverse-phase HPLC (0.1% TFA and a 5–100% CH<sub>3</sub>CN gradient over 30 min on a C8 preparative column). Fractions containing pure product were lyophilized to yield **C10-Y<sup>3+</sup>** as a white solid. Yield: 2 mg (34%, based on a tris(trifluoroacetate) salt). <sup>1</sup>H NMR (400 MHz, D<sub>2</sub>O)  $\delta$  9.00 (s, 1H), 7.37 (m, 7H), 7.24 (m, 8H), 7.13 (d,  $J$  = 7.6 Hz, 2H), 4.82 (m, 3H), 4.30 (m, 1H), 4.05 (s, 2H), 3.69 (d,  $J$  = 16.6 Hz, 1H), 3.45 (t,  $J$  = 13.9 Hz, 2H), 3.15 (m, 5H), 2.76 (d,  $J$  = 14.2 Hz, 1H), 2.68–2.52 (m, 3H), 2.24–2.48 (m, 6H), 2.10 (m 3H), 1.79 (t,  $J$  = 13.0 Hz, 1H), 1.63 (t,  $J$  = 13.5 Hz, 1H), 1.40–1.48 (m, 9H) (see Figure S1). For HRMS, see Figure S2. Additional lanthanide complexes were formed in an analogous way.

**Tag Stability.** Liu et al. reported that their  $\alpha$ -bromoacetamide-containing **CLaNP-9** tag is unstable during lyophilization and that the tag was immediately used for protein labeling following purification.<sup>9</sup> In our hands, lyophilization of purified **C10-Ln<sup>3+</sup>** solutions resulted in a 10% impurity within the lyophilized material, according to analytical HPLC (254 nm), with LC-MS analysis indicating hydrolysis of the bromoacetamide C-Br bond. The amount of hydrolyzed product did not change when an aliquot of a stock solution of lyophilized **C10-Tm<sup>3+</sup>** in H<sub>2</sub>O was left at room temperature for 48 h (Figure S3). Nevertheless, tag stocks were kept frozen at -20 °C when not in use. As the hydrolysis product is unreactive, we proceeded to use the lyophilized complexes for tagging.

**Tagging Reactions.** To a 5 mM DMSO solution of **C10** (about 2.6 mg) loaded with either a paramagnetic lanthanide ion (Tm<sup>3+</sup> or Tb<sup>3+</sup>) or diamagnetic yttrium (Y<sup>3+</sup>) was added an equal volume of 1 mM solution of the PT oligonucleotide in H<sub>2</sub>O. Each solution was then diluted 3-fold by transfer into a mixture of 3:2 (v/v) TEAA (pH 7.5) and DMF. The ligation reaction was conducted at room temperature overnight. Excess tag and unligated DNA were removed by HPLC purification, using a semi-preparative C18 HPLC column with a linear MeOH gradient (30–100%) in 40 mM ammonium carbonate (pH 8.0). Prior to concentrating by lyophilization, the buffer of the DNA fractions was exchanged for water by ultrafiltration.

**Formation of Duplex DNA.** Double-stranded DNA was formed by combining equimolar amounts of single-stranded DNA in NMR buffer (50 mM sodium phosphate, pH 7.4) at room temperature.



**NMR Experiments.** All NMR spectra were recorded at 10 °C on a Bruker 800 MHz NMR spectrometer equipped with a cryoprobe using 50  $\mu$ M solutions of DNA duplex in 3 mm NMR tubes. 2D NOESY spectra were recorded overnight.

**$\Delta\chi$  Tensor Fits.** Pseudocontact shifts were measured as the chemical shift of samples tagged with a paramagnetic lanthanide ( $\text{Tm}^{3+}$  and  $\text{Tb}^{3+}$ ) minus the corresponding chemical shift with a diamagnetic metal ( $\text{Y}^{3+}$ ). The experimental PCS values were used to fit magnetic susceptibility anisotropy ( $\Delta\chi$ ) tensors to a model of double-stranded B-type DNA using the program Numbat.<sup>27</sup> The DNA coordinates were generated using the webserver of the Supercomputing Facility for Bioinformatics & Computational Biology at the Indian Institute of Technology Delhi (<http://www.scfbio-iitd.res.in/software/drugdesign/bdna.jsp>), which uses parameters based on fibre diffraction studies.<sup>26</sup>

**$\Delta\chi$  Tensor Determinations for Ubiquitin with C10-Ln<sup>3+</sup> Tags.** Uniformly <sup>15</sup>N-labeled samples of the ubiquitin mutant A28C were prepared and purified as described previously.<sup>34</sup> Samples were ligated with the C10 tag loaded with either  $\text{Tb}^{3+}$ ,  $\text{Tm}^{3+}$ ,  $\text{Yb}^{3+}$ , or  $\text{Y}^{3+}$ , and  $\Delta\chi$  tensors were determined from <sup>15</sup>N-HSQC spectra as described in the Supporting Information.

## ASSOCIATED CONTENT

### Supporting information

The Supporting Information is available free of charge on the ACS Publications website at DOI:...

<sup>1</sup>H-NMR spectrum of C10-Y<sup>3+</sup>; High-resolution mass spectrum of C10-Y<sup>3+</sup> and predicted *m/z* values; Analytical HPLC traces of purified and lyophilized C10-Tm<sup>3+</sup>; HPLC analysis of SVP digestion of the *R<sub>P</sub>* and *S<sub>P</sub>* diastereomers; HPLC analysis of *S<sub>P</sub>*-DNA following ligation with the C10 tag; Pseudocontact shifts measured for the *R<sub>P</sub>*-PT 14-mer with C10 tag; Pseudocontact shifts measured for the *S<sub>P</sub>*-PT 14-mer with C10 tag; Analysis of the C10 tag using ubiquitin A28C; <sup>15</sup>N-HSQC spectra of ubiquitin A28C with the C10 tag; Correlations between back-calculated and experimental PCSs for C10-tagged ubiquitin A28C; Metal ion position in C10-tagged ubiquitin A28C;  $\Delta\chi$  tensor parameters for C10-tagged ubiquitin A28C; Experimental PCSs for C10-tagged ubiquitin A28C (PDF)

## ACKNOWLEDGMENT

Financial support by the Australian Research Council (grants DP150100383 and FT130100838) is gratefully acknowledged.

## REFERENCES

- (1) Otting, G. (2008) Prospects for lanthanides in structural biology by NMR, *J. Biomol. NMR* 42, 1–9.
- (2) Koehler, J., and Meiler, J. (2011) Expanding the utility of NMR restraints with paramagnetic compounds: Background and practical aspects, *Prog. NMR Spectrosc.* 59, 360–389.
- (3) Liu, W.-M., Overhand, M., and Ubbink, M. (2014) The application of paramagnetic lanthanoid ions in NMR spectroscopy on proteins, *Coord. Chem. Rev.* 273–274, 2–12.
- (4) Nitsche, C., and Otting, G. (2017) Pseudocontact shifts in biomolecular NMR using paramagnetic metal tags. *Prog. NMR Spectrosc.*, 98–99, 20–49.
- (5) Feintuch, A., Otting, G., and Goldfarb, D. (2015) Gd<sup>3+</sup> spin labeling for measuring distances in biomacromolecules: why and how? *Methods Enzymol.* 563, 415–457.
- (6) Su, X.-C., and Otting, G. (2010) Paramagnetic labeling of proteins and oligonucleotides for NMR. *J. Biomol. NMR* 46, 101–112.
- (7) Li, Q.-F., Yang, Y., Maleckis, A., Otting, G., and Su, X.-C. (2012) Thiol-ene reaction: a versatile tool in site-specific labeling of proteins with chemically inert tags for paramagnetic NMR. *Chem. Commun.* 48, 2704–2706.
- (8) Yang, Y., Li, Q.-F., Cao, C., Huang, F., and Su, X.-C. (2013) Site-specific labeling of proteins with a chemically stable, high-affinity tag for protein study. *Chem. Eur. J.* 19, 1097–1103.
- (9) Liu, W.-M., Skinner, S. P., Timmer, M., Blok, A., Hass, M. A., Filippov, D. V., Overhand, M., and Ubbink, M. (2014) A two-armed lanthanoid-chelating paramagnetic NMR probe linked to proteins via thioether linkages, *Chem. Eur. J.* 20, 6256–6258.
- (10) Yang, Y., Wang, J. T., Pei, Y. Y., and Su, X.-C. (2015) Site-specific tagging proteins via a rigid, stable and short thioether tether for paramagnetic spectroscopic analysis, *Chem. Commun.* 51, 2824–2827.
- (11) Chen, J.-L., Wang, X., Yang, F., Cao, C., Otting, G., and Su, X.-C. (2016) 3D structure determination of an unstable transient enzyme intermediate by paramagnetic NMR spectroscopy, *Angew. Chem. Int. Ed.* 55, 13744–13748.
- (12) Schiemann, O., Piton, N., Plackmeyer, J., Bode, B. E., Prisner, T. F., Engels, J.

- W. (2007) Spin labeling of oligonucleotides with the nitroxide TPA and use of PELDOR, a pulse EPR method, to measure intramolecular distances. *Nat. Prot.* 2, 904–923.
- (13) Klakamp, S. L., and Horrocks, W. (1992) Lanthanide ion luminescence as a probe of DNA structure. 2. Non-guanine-containing oligomers and nucleotides. *J. Inorg. Biochem.* 46, 193–205.
- (14) Franklin, S. J. (2001) Lanthanide-mediated DNA hydrolysis. *Curr. Opin. Chem. Biol.* 5, 201–208.
- (15) Eckstein, F. (2000) Phosphorothioate oligodeoxynucleotides: what is their origin and what is unique about them? *Antisense Nucleic Acid Drug Dev.* 10, 117–121.
- (16) Frey, P. A., and Sammons, R. D. (1985) Bond order and charge localization in nucleoside phosphorothioates. *Science* 228, 541–545.
- (17) Fidanza, J. A., Ozaki, H., and McLaughlin, L. W. (1992) Site-specific labeling of DNA sequences containing phosphorothioate diesters. *J. Am. Chem. Soc.* 114, 5509–5517.
- (18) Shepherd, N. E., Gamsjaeger, R., Vandevenne, M., Cubeddu, L., and Mackay, J. P. (2015) Site directed nitroxide spin labeling of oligonucleotides for NMR and EPR studies. *Tetrahedron* 71, 813–819.
- (19) Burgers, P. M. J., and Eckstein, F. (1978) Absolute configuration of the diastereomers of adenosine 5'-O-(1-thiotriphosphate): consequences for the stereochemistry of polymerization by DNA-dependent RNA polymerase from *Escherichia coli*. *Proc. Natl. Acad. Sci. USA* 75, 4798–4800.
- (20) Burgers, P. M. J., Eckstein, F., and Hunneman, D. H. (1979) Stereochemistry of hydrolysis by snake-venom phosphodiesterase. *J. Biol. Chem.* 254, 7476–7478.
- (21) Frederiksen, J. K., and Piccirilli, J. A. (2009) Separation of RNA phosphorothioate oligonucleotides by HPLC. *Methods Enzymol.* 468, 289–309.
- (22) Müller, M., Affolter, M., Leupin, W., Otting, G., Wüthrich, K., and Gehring, W. J. (1988) Isolation and sequence-specific DNA binding of the *Antennapedia* homeodomain. *EMBO J.* 7, 4299–4304.
- (23) Otting, G., Qian, Y. Q., Billeter, M., Müller, M., Affolter, M., Gehring, W. J., and Wüthrich, K. (1990) Protein-DNA contacts in the structure of a homeodomain-DNA complex determined by nuclear magnetic resonance spectroscopy in solution. *EMBO J.* 9, 3085–3092.
- (24) Graham, B., Loh, C.-T., Swarbrick, J. D., Ung, P., Shin, J., Yagi, H., Jia, X.,

- Chhabra, S., Pintacuda, G., Huber, T., et al. (2011) A DOTA-amide lanthanide tag for reliable generation of pseudocontact shifts in protein NMR spectra. *Bioconjugate Chem.* 22, 2118–2125.
- (25) Loh, C.-T., Ozawa, K., Tuck, K., Barlow, N., Huber, T., Otting, G., and Graham, B. (2013) Lanthanide tags for site-specific ligation to an unnatural amino acid and generation of pseudocontacts shifts in proteins. *Bioconjugate Chem.* 24, 260–268.
- (26) Abdelkader, E. H., Lee, M. D., Feintuch, A., Ramirez Cohen, M., Swarbrick, J. D., Otting, G., Graham, B., and Goldfarb, D. (2015) A new Gd<sup>3+</sup> spin label for Gd<sup>3+</sup>-Gd<sup>3+</sup> distance measurements in proteins produces narrow distance distributions. *J. Phys. Chem. Lett.* 6, 5016–5021.
- (27) Schmitz, C., Stanton-Cook, M. J., Su, X.-C., Otting, G., and Huber, T. (2008) Numbat: an interactive software tool for fitting  $\Delta\chi$ -tensors to molecular coordinates using pseudocontact shifts. *J. Biomol. NMR* 41, 179–189.
- (28) Shishmarev, D., and Otting, G. (2013) How reliable are pseudocontact shifts induced in proteins and ligands by mobile paramagnetic tags? A modelling study *J. Biomol. NMR* 56, 203–216.
- (29) Gochin, M. (1998) Nuclear magnetic resonance characterization of a paramagnetic DNA-drug complex with high spin cobalt; assignment of the <sup>1</sup>H and <sup>31</sup>P NMR spectra, and determination of electronic, spectroscopic and molecular properties. *J. Biomol. NMR* 12, 243–257.
- (30) Browne, K. A. (2002) Metal ion-catalyzed nucleic acid alkylation and fragmentation. *J. Am. Chem. Soc.* 124, 7950–7962.
- (31) Shafik, M. T., Bradway, D., Biros, F. J., and Enos, H. F. (1970) Characterization of alkylation products of diethyl phosphorothioate. *J. Agr. Food Chem.* 18, 1174–1175.
- (32) Qin, P. Z., Butcher, S. E., Feigon, J., and Hubbell, W. L. (2001) Quantitative analysis of the isolated GAAA tetraloop/receptor interaction in solution: a site-directed spin labeling study. *Biochemistry* 40, 6929–6936.
- (33) Arnott, S., Campbell-Smith, P. J., and Chandrasekaran, R. (1976) In Handbook of Biochemistry and Molecular Biology, 3rd ed. Nucleic Acids - Volume II, Fasman GP, Ed. Cleveland: CRC Press, pp. 411–422.
- (34) Swarbrick, J. D., Ung, P., Chhabra, S., and Graham, B. (2011) An iminodiacetic acid based lanthanide binding tag for paramagnetic exchange NMR spectroscopy. *Angew. Chem. Int. Ed.* 50, 4403–4406.